Available online at www.sciencedirect.com

SCIENCE DIRECT®

Materials Science and Engineering C 25 (2005) 509 – 515

MATERIALS SCIENCE & ENGINEERING C

www.elsevier.com/locate/msec

Bioconductivity and mechanical properties of plasma-sprayed dicalcium silicate/zirconia composite coating

Youtao Xie[a,b], Xuanyong Liu[a,b], Chuanxian Ding[a], Paul K. Chu[b,*]

[a]*Shanghai Institute of Ceramics, Chinese Academy of Science, 1295 Dingxi Road, Shanghai 200050, China*
[b]*Department of Physics and Materials Science, City University of Hong Kong, Tat Chee Avenue, Kowloon, Hong Kong, China*

Received 7 September 2004; received in revised form 22 October 2004; accepted 25 March 2005
Available online 12 May 2005

Abstract

Dicalcium silicate (C_2S)/yttria stabilized zirconia (YSZ) composite coatings possessing better durability and more superior mechanical properties than pure C_2S coatings were produced by atmospheric plasma spraying. The microstructure and phase composition of the composite coatings were determined by scanning electron microscopy and X-ray diffraction. The bioconductivity of the coatings was evaluated in vitro by incubating in simulated body fluids (SBF). Apatite was observed to precipitate even on coatings comprising more than 70% YSZ after immersion in SBF for 7 days. The changes of the mechanical properties of the composite coatings due to immersion in SBF were also investigated. The durability was found to increase with a larger YSZ content in the coatings. Deterioration of the mechanical properties can be attributed to the degraded interlamellar or cohesive bonding due to fast dissolution of C_2S. This study reveals factors affecting the durability of the C_2S/YSZ composite coatings in simulated physiological environment and suggests means for improvement to address clinical needs.

Keywords: Dicalcium silicate; Yttria stabilized zirconia; Composite coating; Plasma spraying; Bioconductivity; Mechanical properties

1. Introduction

Plasma-sprayed dicalcium silicate (C_2S) coatings exhibit excellent bioconductivity and are promising medical materials in artificial bones and dental roots [1]. A general mechanism on the bioconductivity of $CaO-SiO_2$ based biomaterials involves the dissolution of calcium ions from the coatings [2] to increase the calcium concentration between the bone and implant. The higher calcium concentration bodes well for the precipitation of apatite on the surface of the implant as well as rapid integration of the implant into the existing bone, giving rise to significant improvements in the healing time as well as quality of life of the patients. However, dissolution may also result in the deterioration of the mechanical properties of the coating. Yang et al. [3] have reported worse mechanical properties of hydroxyapatite (HA) coatings after immersion in simulated body fluids (SBF) due to degradation of the interlamellar or cohesive bonding in the coating. The problem stems from the increased porosity after immersion thereby weakening the bonding between the coating and substrate. Fractures have thus been reported to occur in the coating and at the coating/substrate interface in implanted prostheses [4]. The stability and adherence of the substrate/coating and coating/bone interfaces strongly affect the performance of the implant, with the former one largely mechanical and the latter one mainly physiochemical in nature [5]. The long-term stability of the coating is more important when the influence of a physiological medium is considered. There is some indication that rapid dissolution of C_2S in a physiological medium may work against the implant and a possible remedy is to form a composite coating with added particles as a second phase.

Yttria stabilized zirconia (YSZ) is often used as reinforcement in many types of ceramics because it has

* Corresponding author. Tel.: +852 27887724; fax: +852 27889549.
E-mail address: paul.chu@cityu.edu.hk (P.K. Chu).

0928-4931/$ - see front matter © 2005 Elsevier B.V. All rights reserved.
doi:10.1016/j.msec.2005.03.002

high strength and enhanced toughening characteristics during crack–particles interactions [6–9]. Kasuga et al. revealed that the strength and fracture toughness of bulk bioglass consisting of zirconia powders as a second phase could be enhanced with a larger amount of zirconia [10]. It was found in subsequent in vivo experiments that strength degradation on the bioglass incorporated with zirconia powders could be mitigated [11]. A sintered composite of HA/zirconia has also been reported to have a positive effect on the enhancement of the mechanical properties of HA [12–14].

The biocompatibility of YSZ is another crucial issue [15]. The effects of ceramic powders such as Al_2O_3 or ZrO_2/Y_2O_3 on permanent cell lives or human differentiated cells have been investigated and cell culturing results show that the materials do not induce any cytotoxicity [16,17]. Osteoblasts are found to proliferate and dense cell layers form in close contact with the zirconia ceramics. SEM observations reveal good spreading and attachment of osteoblasts onto the material surfaces. Such adhesive properties are regarded to be important to cell proliferation and differentiation into bone forming cells [18].

In this study, YSZ (with 8 wt.% Y_2O_3) was used to reinforce C_2S coatings. The influence of the addition of zirconia on the composite coatings including the effects on the bioconductivity, mechanical properties and durability of the composite coatings were investigated. The YSZ particles were found to reduce the dissolution of the composite coatings and enhance the mechanical properties in terms of the microhardness, Young's modulus, and so on.

2. Experimental

2.1. Materials preparation and plasma spraying

C_2S particles with dimensions of less than 20 μm synthesized in our laboratory and commercially available YSZ powders (typical size ranging from 50 to 106 μm) were used in our experiments. The ceramic slurry method [19] was used to prepare the 50 wt.% C_2S/50 wt.% YSZ (denoted as CZ5), 30 wt.% C_2S/70 wt.% YSZ (denoted as CZ7) and 10 wt.% C_2S/90 wt.% YSZ (denoted as CZ9) composite powders. An atmospheric plasma spraying (APS) system (Sulzer Metco, Switzerland) was employed to fabricate the coatings.

The samples tested for the bioconductivity, microstructure, microhardness and phase composition were fabricated on Ti–6Al–4V plates with dimensions of 10 mm × 12 mm × 2 mm. For the measurements of the bending strength and Young's modulus, a 1.5-mm-thick coating was deposited on steel substrate (150 mm × 100 mm × 2 mm). After plasma spraying, the substrates were removed and the coatings were ground carefully and cut into 25 mm (length) × 4 mm (width) × 1 mm (height) pieces for the standard three-point bending test (ASTM E-855) [20].

2.2. Coating characterization

The structure and phase composition of the coatings were determined by X-ray diffraction (D/max 2550 v, JAPAN) using an angle resolution of 0.02° and the Cu-Ká X-ray line. The surface morphology was evaluated by scanning electron microscopy (SEM) using a JEOL JSM-6700F. The cross-sections of the composite coatings before and after immersion in SBF were polished using Al_2O_3 abrasive powders and diamond grinding paste prior to the analysis of the microstructure and Vickers microhardness. The cross-sectional microstructure of the coatings was studied using scanning electron microscopy and electron probe micro-analysis (EPMA-8705QH$_2$).

The mechanical properties of the specimens before and after immersion in SBF for different durations of time were measured to evaluate the effects of the SBF on the coating properties. A Model HX-1000 microhardness tester made in Shanghai, China was employed to measure the Vickers microhardness. A load of 1.961 N (200 g) was applied for 15 s during indentation and the average values of 20 tests are reported here. The three-point bend strength of the specimens with dimensions of 25 mm (length) × 4 mm (width) × 1 mm (height) was measured using a material testing instrument (Instron-5566, UK). The Young's modulus was obtained by the relationship: $E = PL/4bh^3\delta$, where E is the Young's modulus, P is the load, L is the span length between support, b is the specimen width, h is the specimen thickness, and δ is the deflection at mid-span. Each measured value of Young's modulus represents an average of three tests.

2.3. Bioconductivity evaluation

The bioconductivity of the composite coatings was appraised in vitro by immersion in SBF. The SBF solution

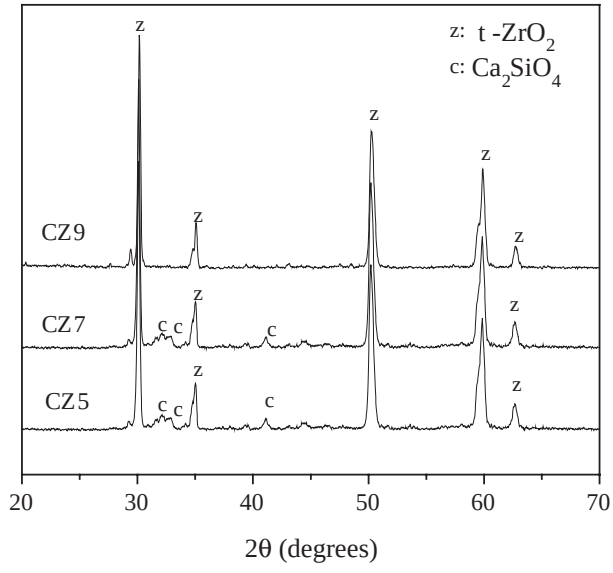

Fig. 1. XRD spectra of the as-sprayed coatings.

was replenished every other day and the samples were incubated in SBF at 36.5 °C for a total of 7 days. Afterwards, the specimens were taken out from the bottles and ultrasonically washed in acetone and deionized water. SEM and energy dispersive X-ray (EDS) analysis (INCA ENERGY, UK) were performed to monitor the formation of apatite.

3. Results and discussion

3.1. Coating characterization

Fig. 1 displays the XRD results acquired from the as-sprayed composite coatings with various ZrO_2 contents and indicates that the coatings are primarily composed of β-Ca_2SiO_4 and t-ZrO_2. A minor amorphous phase is also observed in the composite coatings. No new phases such as $CaZrO_3$ are found in the as-sprayed composite coatings, suggesting that there is no chemical reaction between C_2S and ZrO_2 during the plasma-spraying process. The C_2S peaks can hardly be observed in the XRD spectra because

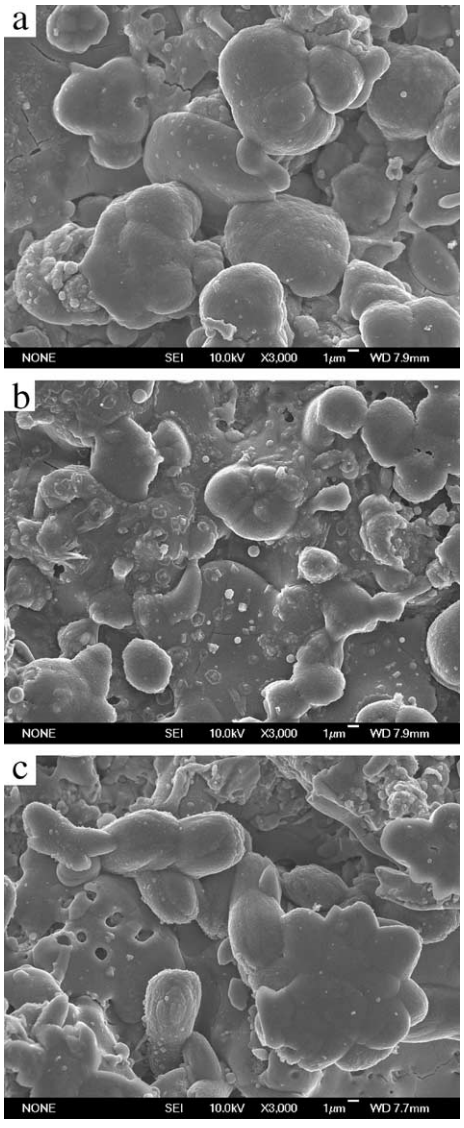

Fig. 2. SEM micrographs of the composite coatings: (a) CZ5, (b) CZ7 and (c) CZ9.

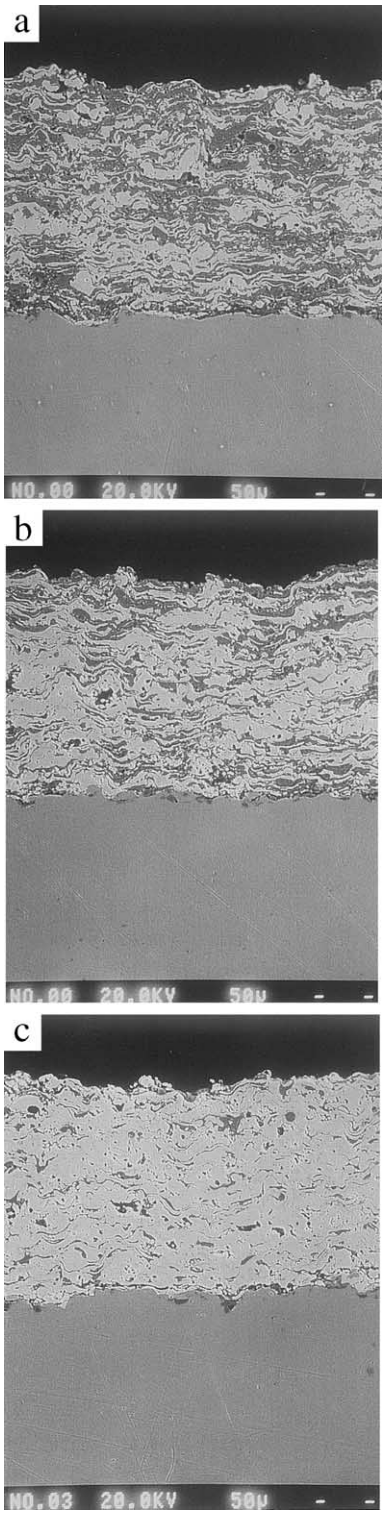

Fig. 3. Cross-sectional view of the as-sprayed composite coatings: (a) CZ5, (b) CZ7 and (c) CZ9.

the peak intensity of ZrO_2 is much higher than that of C_2S. Monoclinic ZrO_2 that exists in the original powder disappears from the as-sprayed coatings and the crystalline γ-Ca_2SiO_4 peaks indicative of the starting powder were substituted by the metastable β-Ca_2SiO_4 phase in the composite coatings. It is believed to be due to rapid solidification in the plasma-spraying process. Tetragonal ZrO_2 remains after plasma spraying and is beneficial to the mechanical properties improvement via stress-induced martensitic transformation to monoclinic phase [21].

Fig. 2 shows the surface morphologies of the composite coatings observed by SEM. There is very little difference among the coatings with different ZrO_2 contents. From the cross-sectional views as shown in Fig. 3, typical lamellar structure of alternating ZrO_2 and C_2S with few pores can be seen. The darker and lighter regions correspond to the C_2S and ZrO_2 phases, respectively. It can be deduced that the ZrO_2 and C_2S particles are distributed uniformly in the coatings without clustering.

3.2. Evaluation of bioconductivity

The surface morphologies of the coatings after immersion in SBF for 7 days are depicted in Fig. 4. New dense layers are found on CZ5 and CZ7. The corresponding EDS spectra indicate that the new layers formed on the surfaces of CZ5 and CZ7 are mainly composed of calcium and phosphorus (Figs. 4d and e). Scattered particles can also be seen on the CZ9 coating surface (Fig. 4c). A higher magnification of the particles is shown at the right corner of CZ9 picture. The scattered particles on the CZ9 surface are also mainly composed of calcium and phosphorus (Fig. 4f). The results show that coating remains bioconductive even with 90 wt.% ZrO_2.

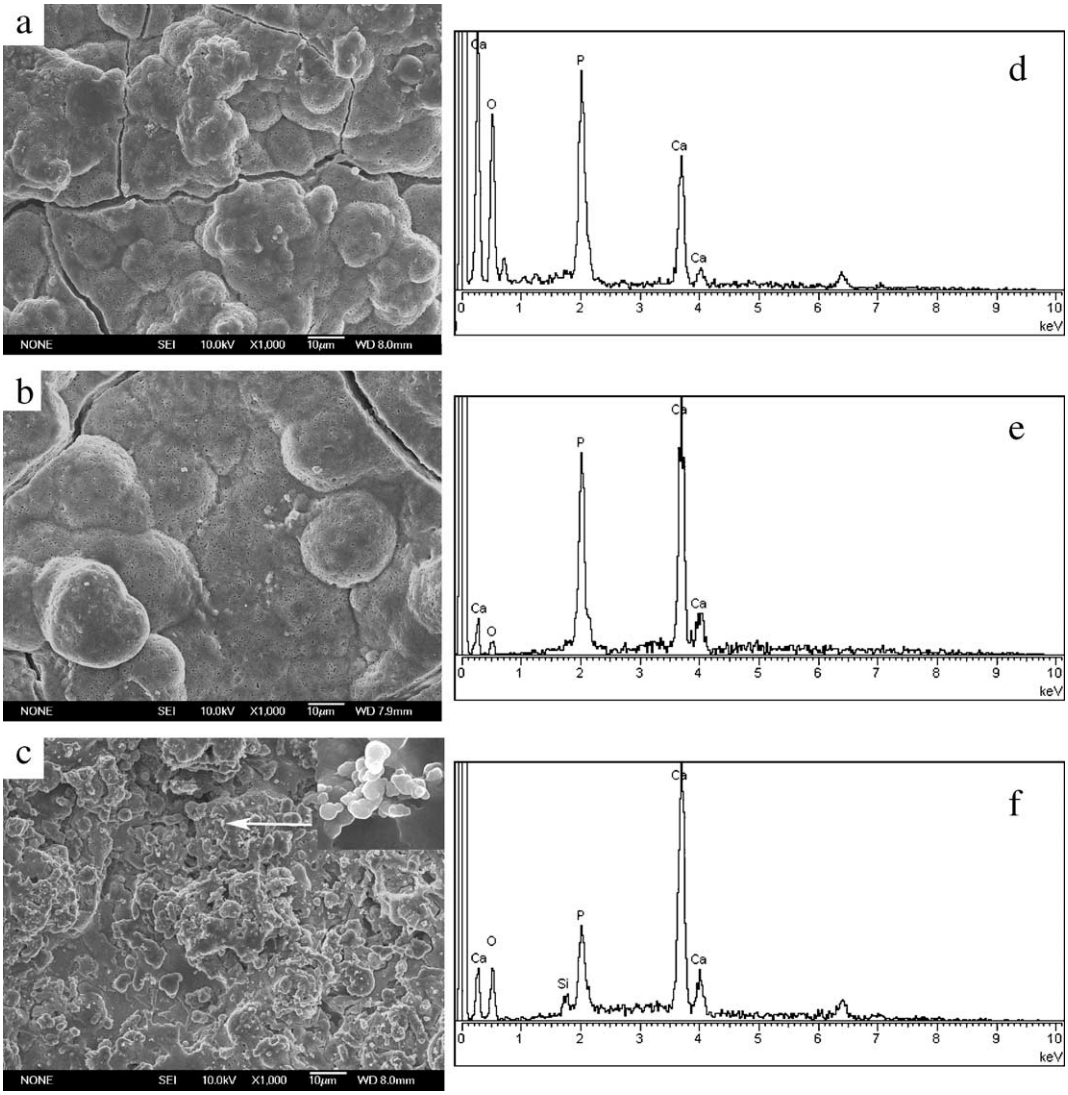

Fig. 4. Surface views of the composite coatings after immersion in SBF for 7 days: (a) CZ5, (b) CZ7, (c) CZ9, (d) EDS spectrum of (a), (e) EDS spectrum of (b), and (f) EDS spectrum of (c).

Fig. 5 depicts the SEM cross-sectional micrographs of CZ5 and CZ7 after immersion in SBF for 28 days. Dense gray layers can be observed on the coating surfaces and the latter analysis confirms that the new layers are apatite.

3.3. Mechanical properties of composite coatings

Fig. 6 shows the microhardness changes of the composite coatings after immersion in SBF for various periods. The higher microhardness of ZrO_2 contributes to the overall microhardness which increases with a higher ZrO_2 content, for instance, from 4.48±0.42 GPa for CZ5 to 6.49±0.27 GPa for CZ9. Dissolution of the C_2S from the composite coatings results in decreased microhardness. The higher the C_2S content in the composite coating, the larger is the decrease in the microhardness after immersion. The microhardness of CZ5 decreases by 37.1% after immersion in SBF for 21 days but that of CZ9 diminishes by only 10.0% after the same incubating period.

The bend strength values of the as-sprayed coatings with different ZrO_2 contents show very little difference (Fig. 7). Although they diminish with longer immersion time, the rate of decrease is smaller than that of other mechanical attributes such as microhardness and Young's modulus. After 21 days of immersion in SBF, the largest decrease of the bend strength of 26% is measured from the CZ5 coating corresponding to a decrease from 117.0±5.4 MPa to 86.7±4.9 MPa.

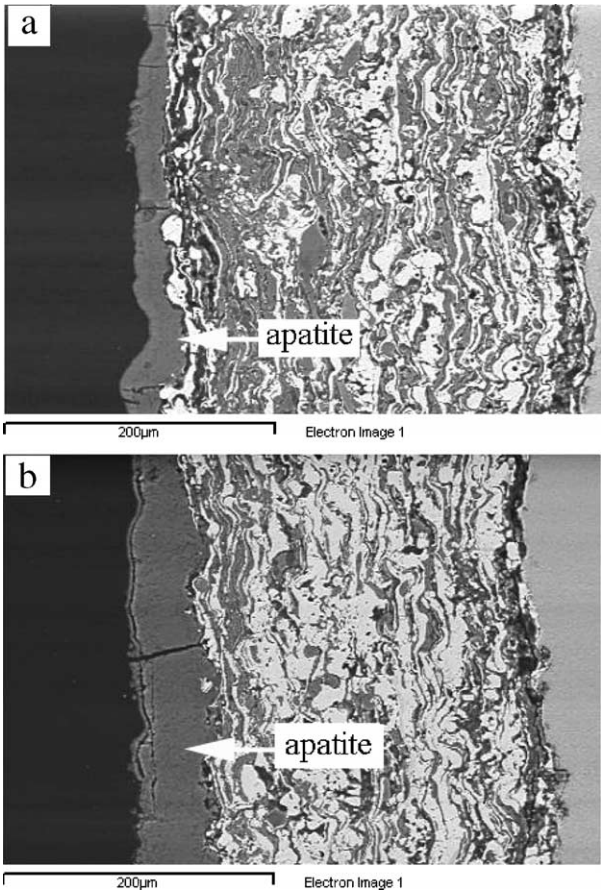

Fig. 5. Cross-sectional views of CZ5 and CZ7 after immersion in SBF for 28 days.

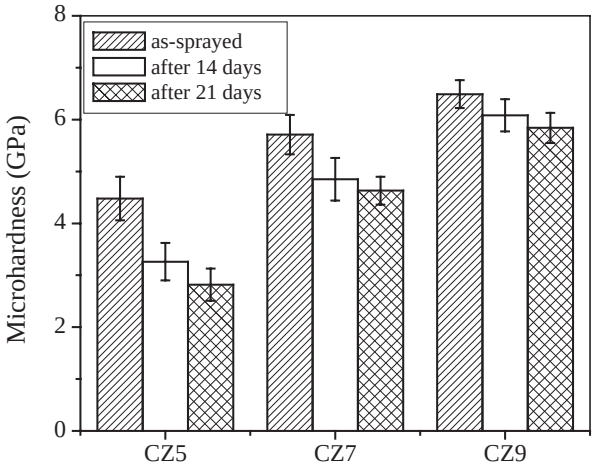

Fig. 6. Microhardness variations of the composite coatings with immersion time in SBF.

The changes in Young's modulus of the composite coatings are illustrated in Fig. 8. Immersion in SBF solution has the largest effects on the Young's modulus of the composite coatings. The modulus of the CZ5 coatings decreases from 107.7±6.8 GPa for the as-sprayed sample to 41.8±3.7 GPa after immersion in SBF for 21 days. The modulus of the CZ7 coatings also goes down from 120.2±9.6 GPa to 56.9±5.8 GPa. The degradation is more than 50% after 3 weeks of immersion. In comparison, CZ9 shows the smallest decrease from 158.4±8.7 GPa (as-sprayed) to 134.7±6.9 GPa (21 days of immersion).

Direct measurement of the Young's modulus of the free coatings detached from the plasma-sprayed coatings by three-point bending testing (ASTE E-855) [20] was attempted by Yang et al. [3]. The effects of SBF on the mechanical properties of the plasma-sprayed hydroxyapatite coatings were studied. Worse Young's modulus results were obtained

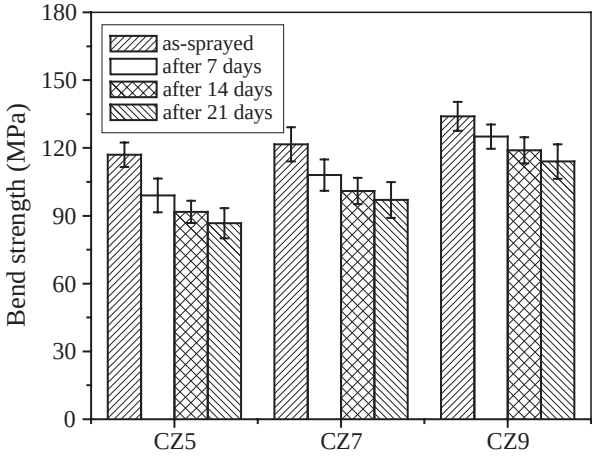

Fig. 7. Bend strength variations of the composite coatings with immersion time in SBF.

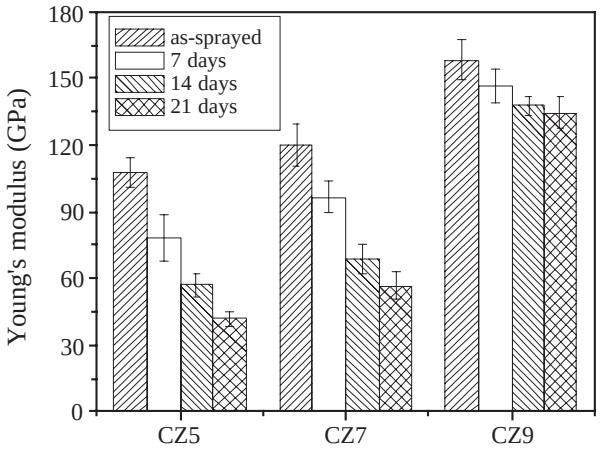

Fig. 8. Young's modulus variations of the composite coatings with immersion time in SBF.

from the hydroxyapatite coatings. The value degraded from 24.1±1.7 GPa for the as-sprayed coatings to 15.6±1.7 GPa after immersion in SBF for 28 days. Khor et al. [19] evaluated the microhardness of the as-sprayed hydroxyapatite coating reinforced with YSZ and Ti–6Al–4V and a value of 400 kg/mm^2 was reported. A Knoop indenter was used to evaluate the Young's modulus of the composite coating and the estimated maximum was about 65 GPa after post-spraying heat treatment. It was also reported that the mechanical properties of the coating increased significantly with the addition of YSZ.

It is demonstrated in this work that the mechanical properties of the C_2S/YSZ composite coatings are improved significantly with the addition of YSZ. The favorable mechanical properties may be ascribed to the existence of YSZ particles as a secondary phase in the coatings. The mechanism is believed to be dispersion strengthening due to homogeneous distribution of YSZ particles in the matrix with a good particle–matrix interface [17]. The ZrO_2 particles used in this work are effectively above the critical size for spontaneous transformation of t-ZrO_2 to m-ZrO_2, although the ZrO_2 typically exists as the tetragonal phase in the composite coatings.

The Young's modulus is a function of structural characteristics such as porosity, crystallinity, and phase composition and that of thermally sprayed coatings is different from that of the bulk materials due to the inhomogeneous microstructure. The phase composition, microcracks and pores in the coatings contribute to the difference in the Young's modulus. The less abundant the ZrO_2 phase (Young's modulus=210 GPa [22], which is much higher than that of C_2S [23]) in the CZ5 coatings, the smaller is the Young's modulus.

C_2S has been found to dissolve rapidly in SBF and so the degradation in the mechanical properties after SBF immersion is primarily caused by dissolution. The dissolution process weakens the interlamellar microstructure in the coating and the interfacial bonding between the coating and substrate. In addition, crack growth may be accelerated by the presence of the physiological environment via processes such as stress-corrosion cracking. Dissolution and crack growth result in weakened interlamellar or cohesive bonding, thereby the poorer mechanical properties. The addition of ZrO_2 results in a slower dissolution rate of the composite coatings and consequently improves the durability and mechanical properties. Our results in fact demonstrate that the higher the ZrO_2 content in the composite coatings, the more stable are the mechanical properties in a simulated physiological environment.

4. Conclusion

Mechanically blended C_2S/YSZ powders were used as feedstock to produce composite coatings by atmospheric plasma spraying. The m-ZrO_2 phase of the original powder disappears and only the t-ZrO_2 can be found in the composite coatings. The crystalline γ-Ca_2SiO_4 phase in the original powder is also replaced by metastable β-Ca_2SiO_4 in the composite coatings. It is because of rapid solidification during the plasma-spraying process. In our SBF incubating tests, coatings composed of as high as 70% of ZrO_2 exhibit very good bioconductivity, and a dense apatite layer can be found on the surface after 7 days of immersion in SBF.

The composite coatings possess enhanced mechanical properties due to the addition of YSZ. The Young's moduli of the as-sprayed composite coating are 107.7±6.8 GPa (CZ5), 120.2±9.6 GPa (CZ7) and 158.4±8.7 GPa (CZ9), respectively. With large amount of YSZ addition, the microhardness and bend strength of the coatings are also improved markedly. The improved mechanical properties of the composite coatings are believed to stem from the homogeneous distribution of ZrO_2 in the coatings. Composite coatings with a higher ZrO_2 content show smaller dissolution, and so the degree of degradation in the mechanical properties is reduced. The durability of the coatings is also enhanced.

Acknowledgements

This work was jointly supported by Shanghai Science and Technology RD Fund under grants 02QE14052 and 03JC14074, Hong Kong Research Grants Council (RGC) Competitive Earmarked Research Grants (CERG) #CityU 1137/03E and CityU 1120/04E, and City University of Hong Kong Strategic Research Grant (SRG) #7001642.

References

[1] X.Y. Liu, S.Y. Tao, C.X. Ding, Bioactivity of plasma sprayed dicalcium silicate coatings, Biomaterials 23 (2002) 963–968.
[2] X.Y. Liu, C.X. Ding, P.K. Chu, Mechanism of apatite formation on wollastonite coatings in simulated body fluids, Biomaterials 25 (10) (2004) 1755–1761.

[3] Y.C. Yang, E. Chang, S.Y. Lee, Mechanical properties and Young's modulus of plasma-sprayed hydroxyapatite coating on Ti substrate in simulated body fluid, J. Biomed. Mater. Res. 67A (2003) 886–889.
[4] B.C. Wang, T.M. Lee, E. Chang, C.Y. Yang, The shear strength and the failure mode of plasma sprayed hydroxyapatite coating to bone: the effect of coating thickness, J. Biomed. Mater. Res. 27 (1993) 1315–1327.
[5] Y.C. Tsui, C. Doyle, T.W. Clyne, Plasma sprayed hydroxyapatite coatings on titanium substrates: Part 1. Mechanical properties and residual stress levels, Biomaterials 19 (1998) 2015–2029.
[6] N. Claussen, Fracture toughness of Al_2O_3 with an unstabilized ZrO_2 dispersed phase, J. Am. Ceram. Soc. 59 (1976) 49–51.
[7] D.J. Green, Critical microstructures for microcracking in Al_2O_3/ZrO_2 composites, J. Am. Ceram. Soc. 65 (1982) 610–614.
[8] M. Ruhle, A.G. Evans, R.M. Mcmeeking, P.G. Charalambides, Microcrack toughening in alumina/zirconia, Acta Metall. 35 (1987) 2701–2710.
[9] B.Y. Chou, E. Chang, S.Y. Yao, J.M. Chen, Phase transformation during plasma spraying of hydroxyapatite–10 wt.%–zirconia composite coating, J. Am. Ceram. Soc. 85 (3) (2002) 661–669.
[10] T. Kasuga, K. Nakajima, T. Uno, M. Yoshida, Preparation of zirconia toughened bioactive glass/ceramic composite by sinter hot isostatic pressing, J. Am. Ceram. Soc. 75 (5) (1992) 113–117.
[11] T. Kasuga, M. Yoshda, A.J. Ikushima, M. Tuchiya, H. Kusakari, Stability of zirconia-toughened bioactive glass/ceramics: in vivo study using dogs, J. Mater. Sci. 4 (1993) 36–39.
[12] J.M. Wu, T.S. Yeh, Sintering of hydroxyapatite/zirconia composite materials, J. Mater. Sci. 23 (1988) 3771–3777.
[13] K. Ioku, S. Somiya, M. Yoshimura, Hydroxyapatite ceramics with tetragonal zirconia particles dispersion prepared by HIP postsintering, J. Jpn. Ceram. Soc. 99 (3) (1991) 196–203.
[14] N. Tamari, M. Mouri, I. Kondo, Mechanical properties and existing phases of composite ceramics obtained by sintering of a mixture of hydroxyapatite and zirconia, J. Jpn. Ceram. Soc. 95 (8) (1987) 806–809.
[15] S.F. Hulbert, in: L.L. Hench, J. Wilson (Eds.), The Use of Alumina and Zirconia in Surgical Implants: An Introduction to Bioceramics, Word Scientific Publishing Co., Singapore, 1993, pp. 25–40.
[16] H. Lang, T.H. Mertens, The use of human osteoblast like cells as an in vitro test system for dental materials, J. Oral Maxillofac. Surg. 48 (1990) 606–611.
[17] I. Dion, L. Bordenave, F. Lefebvre, R. Bareille, C. Baquey, J.R. Monties, P. Havlik, Physico-chemistry and cytotoxicity of ceramics, J. Mater. Sci. 5 (1994) 18–24.
[18] U. Meyer, D.H. Szulczewski, R.H. Barckhaus, M. Atkinson, D.B. Jones, Biological evaluation of an ionomeric bone cement by osteoblast cell culture methods, Biomaterials 14 (1993) 917–924.
[19] K.A. Khor, Y.W. Gu, D. Pan, P. Cheang, Microstructure and mechanical properties of plasma sprayed HA/YSZ/Ti–6Al–4V composite coatings, Biomaterials 25 (18) (2004) 4009–4017.
[20] ASTM E-855-90, Standard Test Methods for Bend Testing of Metallic Flat Materials for Sparing Applications Involving Static Loading, American Society for Testing Materials, West Conshohocken, PA, 1990.
[21] T.K. Gupta, J.H. Bechtold, R.C. Kuznicki, L.H. Cadoff, Stabilization of tetragonal phase in polycrystalline zirconia, J. Mater. Sci. 12 (12) (1977) 2421–2426.
[22] N. Bambaa, Y.H. Choab, T. Sekinoc, K. Niiharac, Mechanical properties and microstructure for 3 mol% yttria doped zirconia/silicon carbide nanocomposites, J. Eur. Ceram. Soc. 23 (2003) 773–780.
[23] I. Nettleship, K.G. Slavick, Y.J. Kim, W.M. Kriven, Phase transformations of dicalcium silicate: I. Fabrication and phase stability of fine grained β-phase, J. Am. Ceram. Soc. 75 (9) (1992) 2407–2419.